Asunto **Your Submission**
Remitente Lech Pawlowski <lech.pawlowski@unilim.fr>
Destinatario epuchi@reacciun.ve <epuchi@reacciun.ve>
Fecha 26.04.2012 11:27

Ms. Ref. No.: SURFCOAT-D-12-00232R1
Title: Fatigue behaviour of AA7075-T6 aluminium alloy coated with a WC-10Co-4Cr cermet by HVOF thermal spray
Surface and Coatings Technology

Dear Eli,

I am pleased to confirm that your paper "Fatigue behaviour of AA7075-T6 aluminium alloy coated with a WC-10Co-4Cr cermet by HVOF thermal spray" has been accepted for publication in Surface and Coatings Technology.

Comments from the Editor and Reviewers can be found below.

Thank you for submitting your work to this journal.

With kind regards,

Lech

Special Issue Managing Guest Editor
Surface and Coatings Technology

Comments from the Editors and Reviewers:

The paper is acceptable now.

Surface & Coatings Technology xxx (2012) xxx–xxx

Contents lists available at SciVerse ScienceDirect

Surface & Coatings Technology

journal homepage: www.elsevier.com/locate/surfcoat

Fatigue behavior of AA7075-T6 aluminum alloy coated with a WC–10Co–4Cr cermet by HVOF thermal spray

E.S. Puchi-Cabrera [a,b,c,*], M.H. Staia [a], Y.Y. Santana [a], E.J. Mora-Zorrilla [d], J. Lesage [c], D. Chicot [c], J.G. La Barbera-Sosa [a], E. Ochoa-Perez [a], C.J. Villalobos-Gutierrez [d]

[a] School of Metallurgical Engineering and Materials Science, Faculty of Engineering, Universidad Central de Venezuela, Postal Address 47885, Los Chaguaramos, Caracas 1041, Venezuela
[b] Venezuelan National Academy for Engineering and Habitat, Palacio de las Academias, Postal Address 1723, Caracas 1010, Venezuela
[c] Université Lille Nord de France, USTL, LML, CNRS, UMR 8107, F-59650 Villeneuve d'Ascq, France
[d] School of Mechanical Engineering, Faculty of Engineering, Universidad Central de Venezuela, Postal Address 47885, Los Chaguaramos, Caracas 1041, Venezuela

ARTICLE INFO

Available online xxxx

Keywords:
Fatigue behavior
7075 aluminum alloy
WC–10Co–4Cr cermet
HVOF thermal spray

ABSTRACT

Rotating bending fatigue experiments, both in air and in a 3% NaCl solution, have been carried out in order to study the fatigue behavior of a 7075-T6 aluminum alloy coated with a WC–10Co–4Cr cermet by high velocity oxygen fuel (HVOF) thermal spray, without any grit blasting prior to the coating deposition. The results indicate that the presence of the coating gives rise to a significant increase in the fatigue strength of the substrate and therefore, that from the fatigue behavior point of view this coating could be a feasible replacement of electrolytic hard chromium plating in aircraft applications. Such an increase in fatigue and corrosion-fatigue strength is believed to be associated with the intrinsic microstructural characteristics, corrosion resistance and mechanical properties of the coating, its compressive residual stresses and the possible compressive residual stress field induced in the substrate during coating deposition. The fractographic analysis of the specimens indicates that the final fatigue fracture could be due either to the joint action of a large number of cracks, which propagate from the substrate–coating interface, or to a single dominant fatigue crack, depending on the maximum alternating stress applied to the coated system. It is shown that the lack of grit blasting prior to HVOF deposition does not seem to compromise the functionality of the coated system, while it avoids the introduction of further sharp stress concentrators for the nucleation of fatigue cracks.

1. Introduction

The significant development experienced in the past few years by the aircraft and aerospace industries has been intimately associated with the improvements in airframe design and the forming processes employed in the manufacture of many different parts and components that constitute these complex structures [1]. Such advances in aircraft and aerospace engineering have also been possible due to the availability of a wide range of alloys with higher mechanical properties, particularly in relation to fatigue, crack propagation and stress corrosion cracking resistance [2].

Among these aeronautical materials, aluminum alloys of the 7000 series, supplied in different forms, have been extensively used for the manufacture of different critical aircraft components subjected to complex stress states, which include upper wing surfaces, internal ribs, spars, frames, landing gear and dynamic helicopter components, among others. The improvement in the mechanical properties of these materials has been possible due to the development and optimization of different thermo-mechanical processes [2].

However, in spite of their excellent bulk mechanical properties, in general, aluminum alloys of the 7000 series have poor surface properties, particularly in relation to applications that require wear and corrosion resistance. This disadvantage has led to the extensive use of hexavalent-chromium-based conversion coatings (HCCC), such as electrolytic hard chromium (EHC) plating and chromic acid anodizing (CAA), in order to improve their surface properties [3–7]. Nevertheless, it is well known that these treatments utilize chemicals that contain hexavalent chromium (Cr^{6+} ions), which is a carcinogenic substance subjected to a strong health and environmental international regulation [8–11].

EHC plating not only gives rise to a significant decrease in the fatigue properties of both ferrous and non-ferrous substrates, which represents a critical aspect for the aeronautic and aircraft industries. Also, it has an unreliable performance, delaminates in service and promotes hydrogen embrittlement in ferrous alloys [12,13].

* Corresponding author at: School of Metallurgical Engineering and Materials Science, Faculty of Engineering, Universidad Central de Venezuela, Postal Address 47885, Los Chaguaramos, Caracas 1041, Venezuela. Université Lille Nord de France, USTL, LML, CNRS, UMR 8107, F-59650 Villeneuve, France. Tel.: +33 7 78 19 09 14.
E-mail addresses: epuchi@reacciun.ve, epuchi@cantv.net (ES. Puchi-Cabrera).

0257-8972/$ – see front matter © 2012 Elsevier B.V. All rights reserved.
doi:10.1016/j.surfcoat.2012.04.087

On the other hand, Camargo et al. [14] have also carried out an investigation on the fatigue behavior of a 7050-T7451 aluminum alloy whose surface was modified by the growth of anodic films, by means of sulfuric and chromic acid anodizing, as well as hard anodizing. Their results showed clearly that in this case, the presence of the films also gives rise to a degradation of the fatigue properties of the substrate. However, they were able to show that shot peening with glass shot prior to anodizing could restore the fatigue performance of the aluminum alloy substrate.

One of the possible alternatives for the replacement of EHC plating, as well as acid and hard anodizing is plasma spray. However, previous studies on the fatigue behavior of 7075-T6 aluminum alloy coated by this process with a WC–12Co cermet, tested under rotating bending conditions, showed that grit blasting and coating of the substrate gave rise to a significant decrease in fatigue properties, regardless of the testing medium (air or a NaCl solution) [15]. As shown in Figs. 1 and 2, even after correcting the specimen diameter, by subtracting the coating thickness, a significant debit in the fatigue properties of the substrate takes place, except when the coated system is tested in a NaCl solution at relatively low maximum alternating stresses.

A similar decrease in fatigue properties has been reported by Sartwell et al. [16], who carried out axial fatigue tests (R = 0.1) on samples of a 7075 aluminum alloy, but coated with WC–Co cermets of 76 and 280 μm in thickness, deposited by HVOF thermal spray. However, these authors were also able to observe a significant increase in the fatigue properties of the substrate alloy when this was coated with a WC–CoCr cermet of 280 μm and with a duplex coating of Triballoy 400 and WC–Co of 76 μm, which were also deposited by means of HVOF.

In this sense, Camargo et al. [14] have also reported an increase in the fatigue strength of a 7050-T7451 aluminum alloy coated with a WC–17%Co cermet of 150 μm deposited by means of HVOF thermal spray. However, a significant decrease in fatigue strength could also occur if the substrate alloyed was shot peened with glass shot of 0.4 mm in diameter, prior to HVOF deposition.

It has been shown that grit blasting with alumina particles prior to HVOF deposition, in order to increase the mechanical bonding of the coating to the substrate, could have a deleterious effect on the fatigue strength of the latter, as a consequence of the increase in roughness and the stress concentrations that arise from the alumina particles embedded into the substrate [16,17].

Given the above results reported by Sartwell et al. [16], the WC–10Co–4Cr cermet represents an interesting possibility for coating aluminum alloys without any prior grit blasting. As it has already been shown by Santana et al. [18], this coating is quite dense and homogeneous, with less than 1% porosity on the deposition surface

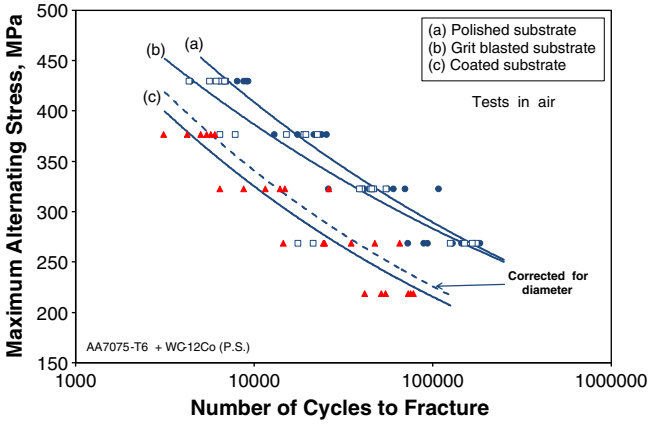

Fig. 1. Number of cycles to fracture as a function of the maximum alternating stress applied to the coated system by plasma spray (P. S.) tested in air.

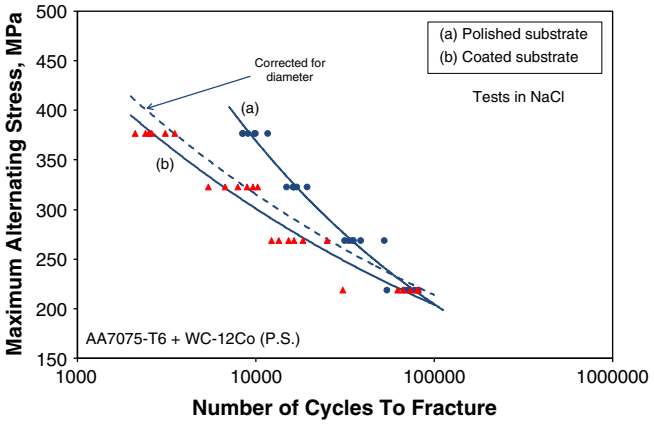

Fig. 2. Number of cycles to fracture as a function of the maximum alternating stress applied to the coated system by plasma spray (P. S.) tested in a 3% NaCl solution.

and less than 0.3% porosity on its cross section. It is composed mainly of WC grains, whose mean grain size is ~1 μm, embedded in a Co matrix. These authors, employing XRD techniques, have also shown that during the deposition of this coating, some WC decarburization could take place, giving rise to the presence of W_2C peaks in the diffraction pattern of the coating.

Santana et al. [18] have also carried out a thorough characterization of the coating hardness both by classical Vickers indentation as well as by continuous loading–unloading micro and nanoindentation. The results of this previous study indicates that the mean coating hardness ranges between ~10 and 14 GPa, with similar hardness values both on the cross section and on the deposition plane.

Regarding its residual stress profile, these authors have also conducted a detailed analysis of it on a coating of approximately 500 μm in thickness, by means of the incremental hole drilling technique [19]. Details of the experimental procedure have been described elsewhere [20] in relation to the evaluation of the residual stresses of the different WC-based coatings deposited by HVOF thermal spray. The results of these studies indicate that the WC–10Co–4Cr cermet is under a compressive residual stress state, as determined from the negative values of the through thickness relaxation strains. Thus, between 150 and 400 μm, the mean value of the in-plane principal stresses was observed to range from ~210 to 30 MPa, in compression. However, at the substrate coating interface, the mean value of the residual stresses achieved a magnitude of ~780 MPa, also in compression.

Thus, given the above facts and the possibility of generating a compressive residual stress field into the substrate material as a consequence of plastic deformation during HVOF deposition, the present investigation has been conducted in order to evaluate the fatigue performance, both in air and in a NaCl solution, of a 7075-T6 aluminum alloy coated with a WC–10Co–4Cr cermet by HVOF thermal spray, without any grit blasting prior to the deposition process and to compare this performance with that of the uncoated substrate.

2. Experimental techniques

2.1. Experimental alloy and sample preparation

The present investigation has been conducted by employing samples of a 7075-T6 aluminum alloy with the following composition (wt.%): 6.10 Zn, 2.90 Mg, 2.00 Cu, 0.50 Fe, 0.40 Si, 0.30 Mn, 0.28 Cr, and Al bal. The material was provided as bars of approximately 12.7 mm in diameter and 3.6 m in length, from which a number of tensile and fatigue specimens were machined following the ASTM standards B557 and E606, respectively. The sketches of both the tensile and fatigue specimens have been reported elsewhere [15].

Please cite this article as: ES. Puchi-Cabrera, et al., Surf. Coat. Technol. (2012), doi:10.1016/j.surfcoat.2012.04.087

Table 1
Geometrical and deposition parameters of the HVOF process.

Nozzle length	100 mm
Spraying distance	150–200 mm
Powder feeding rate	1.38 g s^{-1}
Range of particle size	~22–66 μm
Kerosene flux	6.22×10^{-3} l s^{-1}
Kerosene pressure	670 kPa
Oxygen flux	11.40 l s^{-1}
Oxygen pressure	1400 kPa
Chamber combustion pressure	620 kPa

The introduction of residual stresses throughout the machining operation of the specimens was minimized by employing adequate lubrication and by reducing continuously the depth of cut of the material during the turning procedure, which required the use of a turret lath at a low speed. All the samples were polished mechanically until the apparent surface roughness (R_a) achieved a value less than 3 μm. For this purpose, SiC papers with grit nos. 400–2000 were employed. In this way, the remaining circumferential notches that could act as stress concentrators during the fatigue tests were eliminated. The roughness of the specimens was measured by means of optical profilometry.

The samples were subsequently coated, without any prior grit blasting, with a WC–10Co–4Cr cermet of approximately 200 μm in thickness, by means of HVOF thermal spraying. This step was accomplished by employing a Praxair-TAFA JP-5000 gun, using a mixture of kerosene, as fuel, and oxygen. The main parameters involved both in the gun geometry and deposition process, are given in Table 1. In the as-deposited condition, the mean roughness of the samples increased significantly and therefore, further mechanical polishing was carried out in order to decrease such parameter to values less than approximately 4 μm. The microstructural characterization of the coatings after mechanical polishing was conducted by means of standard SEM and EDS techniques.

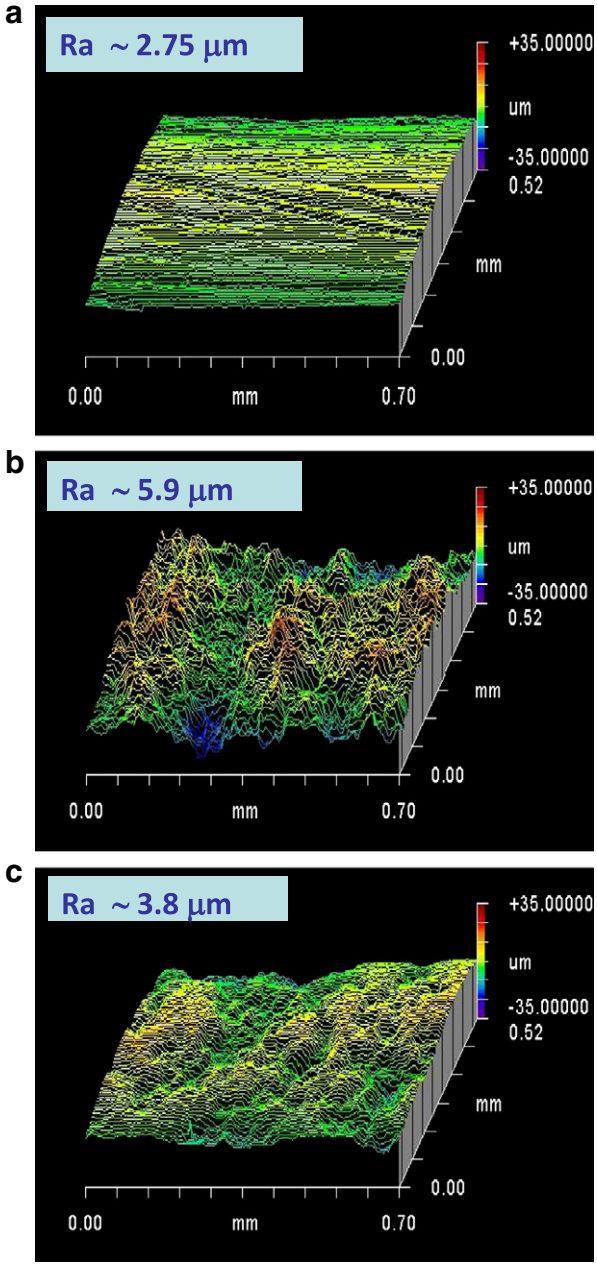

Fig. 3. Apparent surface roughness of the specimens: (a) prior to HVOF deposition, (b) after coating and (c) after mechanical polishing subsequent to deposition of the coating, prior to fatigue testing.

2.2. Mechanical testing of the coated system

The static mechanical properties of the coated system were evaluated by means of tensile testing, employing a MTS 810 servo-hydraulic equipment. Five tensile samples were employed for this purpose. Fatigue tests were carried under rotating bending conditions ($R = -1$), employing a Fatigue Dynamics RBF-200 equipment at a frequency of 50 Hz. Tests were conducted at maximum alternating stresses in the range of 125–323 MPa, employing not less than 25 specimens for each testing condition. After fatigue testing, a detailed SEM fractographic analysis of some selected samples was carried out. This study was conducted with the purpose of characterizing the failure mechanisms that took place during fatigue testing, identifying the fatigue crack initiation sites and determining the different mechanisms of crack propagation that predominate in this particular coated system. To accomplish this objective, a Philips XL30 microscope under a back scattered electron mode was employed. The observations were made both on the fracture surface of the specimens and on cross sections normal to the fracture plane.

3. Experimental results

3.1. Microstructural characterization of the coated system

Fig. 3a through c illustrates the apparent surface roughness (R_a) of the specimens prior to HVOF deposition, after coating and after

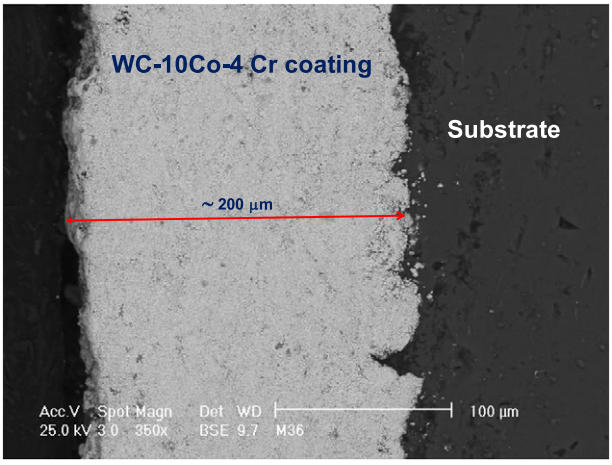

Fig. 4. SEM cross section view of the coated system. It can be observed that the mean coating thickness is ~200 μm.

Please cite this article as: ES. Puchi-Cabrera, et al., Surf. Coat. Technol. (2012), doi:10.1016/j.surfcoat.2012.04.087

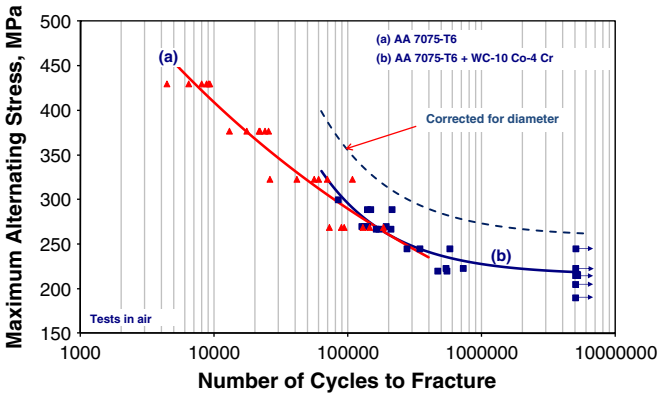

Fig. 5. Number of cycles to fracture as a function of the maximum alternating stress applied to the investigated coated system tested in air.

mechanical polishing subsequent to deposition of the coating, prior to fatigue testing. Before HVOF deposition, R_a is less than ~3 μm, which increases up to ~6 μm after coating. Final polishing prior to fatigue testing gave rise to a reduction in R_a to less than ~4 μm. On the other hand, Fig. 4 illustrates a SEM cross section view of the coated system and it is shown that the mean coating thickness is 200 ± 10 μm. Also, one can clearly observe the highly irregular profile of the substrate–coating interface, as a consequence of the plastic deformation of the substrate induced by the impact of the coating particles.

3.2. Fatigue behavior of the substrate–coating system

Figs. 5 and 6 summarize the results obtained regarding the fatigue behavior of the coated system when the tests are conducted both in air and in a 3% NaCl solution. The above figures also present a comparison of the coated system behavior and that of the uncoated substrate tested under similar conditions and reported elsewhere [21], whose data has been extended, in the present investigation, to a greater number of cycles to fracture. The points in Figs. 5 and 6 represent the experimental data and due to the trend exhibited by the tested materials, these have been described by means of the simple parametric relationship earlier proposed by Stromeyer [22]:

$$S = S_L + BN_f^{-m}, \text{MPa}. \quad (1)$$

In this expression, S_L represents the fatigue limit, whereas B and m represent material constants, all of which are determined from the experimental S–N data. The values of the parameters involved in Eq. (1) for the uncoated and coated substrates tested under different conditions, are presented in Table 2.

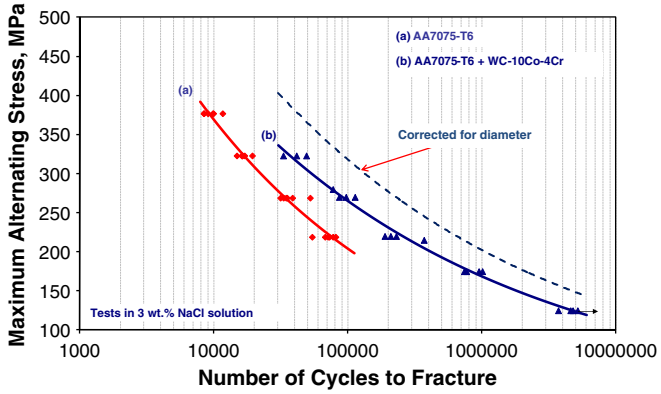

Fig. 6. Number of cycles to fracture as a function of the maximum alternating stress applied to the investigated coated system tested in a 3% NaCl solution.

Table 2
Parameters involved in the Stromeyer relationship [Eq. (1)] for the tested materials.

Material condition	S_L, MPa	B, MPa	m
Uncoated substrate tested in air	116.6	2237.2	0.22
Uncoated substrate tested in NaCl	101.1	8002.0	0.37
Coated system tested in air	198.5	90,730	0.6
Coated system tested in air (corrected for diameter)	258.2	1.17×10^6	0.82
Coated system tested in NaCl	19.9	3136.4	0.22
Coated system tested in NaCl (corrected for diameter)	10.2	3250.8	0.21

The dotted lines included in Figs. 5 and 6 represent the fatigue behavior of the coated system, after correcting the diameter of the samples, by subtracting the coating thickness, for the re-computation of the maximum alternating stress on the basis of the diameter of the machined specimens. Therefore, it is assumed that the coating does not act as a load-carrying element of the system, as it is usually considered in similar fatigue testing programs [12,13].

By comparing the corrected fatigue curves with those of the uncoated substrate, for each testing medium, it can be clearly observed that the deposition of the WC–10Co–4Cr cermet onto this aluminum alloy gives rise to a significant increase in the fatigue properties of the substrate. When the coated system is tested in air,

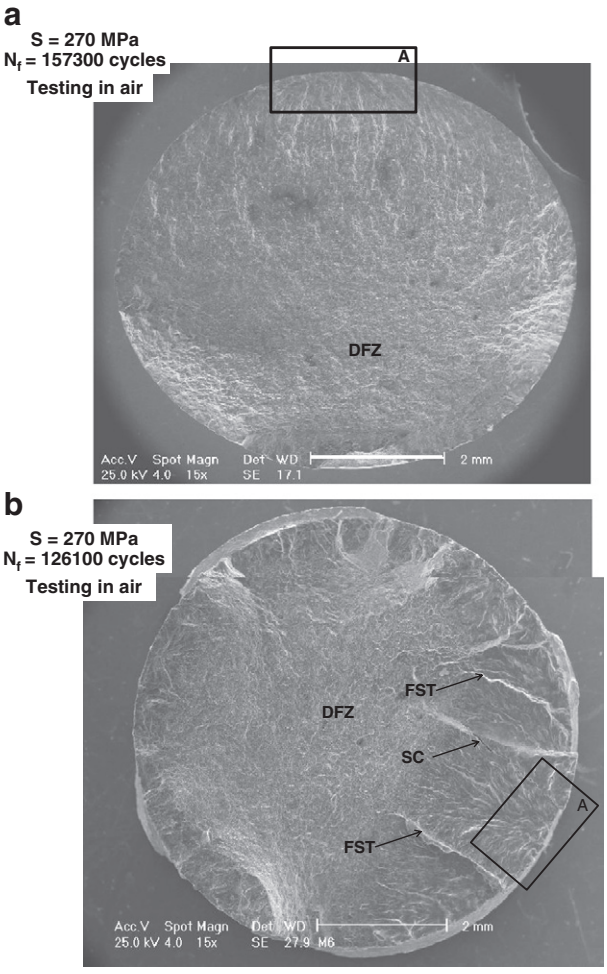

Fig. 7. (a) Fracture surface of an uncoated sample tested in air, which failed after 157,300 cycles at a maximum alternating stress of 270 MPa. (b) Fracture surface of a coated sample tested in air, which failed after 126,100 cycles at a maximum alternating stress of 270 MPa. The fracture of the specimen in b occurred as a consequence of the nucleation and simultaneous propagation of a number of cracks, possibly initiated at the substrate coating interface.

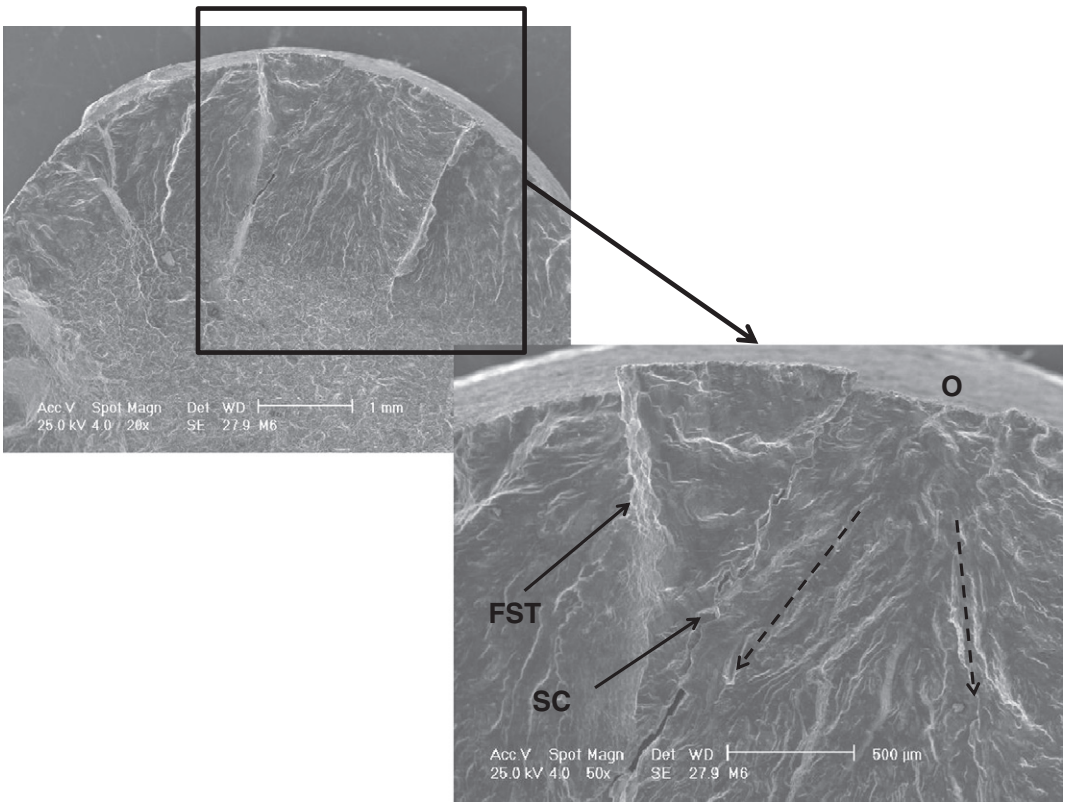

Fig. 8. Magnified view of one of the crack initiation sites identified as A in Fig. 7b. The dotted arrows indicate the propagation direction of a crack nucleated at site O.

in the range of 10^5–10^6 cycles to fracture, the mean increase in the fatigue strength of the substrate is ~19%. In fact, if testing is conducted at maximum alternating stresses below ~215 MPa, the specimens can achieve more than 5×10^6 cycles without fracture. Similarly, when the coated system is tested in the NaCl solution, the increase in the fatigue strength of the substrate, for the same interval of cycles to fracture, is observed to be much higher and to vary from ~35 to 47%. It is noticeable that under such severe testing conditions, at maximum alternating stresses of 125 MPa, the specimens are also able to achieve ~5×10^6 cycles before fracture.

3.3. Fractographic analysis

A detailed fractographic analysis of some of the uncoated and coated specimens tested both in air and in the NaCl solution was carried out, in order to understand better the fracture mechanisms in this coated system, in comparison with the uncoated substrate. Particularly, in the case of the coated specimens, which due to the presence of the coating were actually tested at maximum alternating stresses ~20% higher than the uncoated samples, it is important to determine if the final fracture occurred due to the nucleation and propagation of a dominant crack or to the simultaneous joint action of a number of cracks, which propagated at a similar rate.

For this purpose, different samples tested at high and low maximum alternating stresses were analyzed both on their fracture surface and along cross sections normal to the latter. Also, cross sections of samples tested in air, which were able to achieve 5×10^6 cycles without fracture, were studied in order to evaluate qualitatively the mechanical integrity of the coating and the state of the substrate–coating interface, after such loading history.

Thus, Fig. 7a and b illustrates the fracture surfaces of both an uncoated specimen and a coated sample tested in air at 270 MPa. As can be clearly observed and as expected, the fracture surfaces exhibit different characteristics. The uncoated sample failed after 157,300 cycles and the fracture surface shows the presence of a single dominant crack whose origin is enclosed in the area identified as A, leading to the

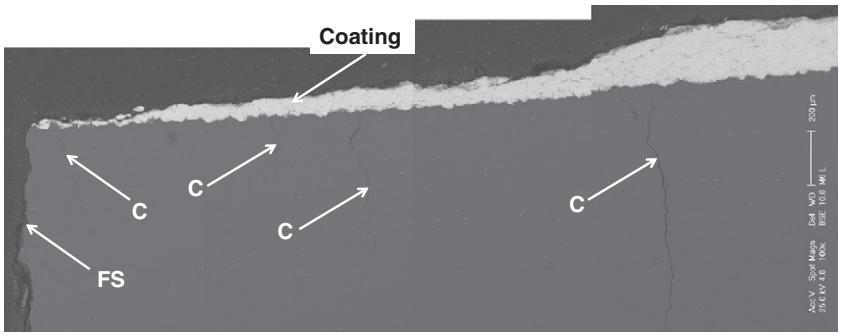

Fig. 9. Cross section view of the specimen shown in Figs. 7b and 8. A number of primary cracks (identified as C), which run parallel to the fracture surface (FS), into the substrate can be observed.

Please cite this article as: ES. Puchi-Cabrera, et al., Surf. Coat. Technol. (2012), doi:10.1016/j.surfcoat.2012.04.087

displacement of the ductile fracture zone (DFZ) to the opposite location of the crack nucleation site. On the contrary, the coated specimen failed after 126,100 cycles and the SEM photomicrograph shows clearly that the fracture of the specimen occurred as a consequence of the nucleation and simultaneous propagation of a number of cracks, possibly initiated at the substrate coating interface. This conclusion is supported by the fact that the DFZ is located at the center of the sample and the existence of numerous fracture steps (FST), which separate the propagation zones of the different cracks that gave rise to the fracture of the specimen, as shown on the photograph. Also, some secondary cracks (SC) initiated at the interface could be observed, indicating that the nucleated cracks are able to bifurcate and change their propagation direction. The analysis of this fracture surface points out that after such loading history, extensive delamination of the coating occurs and that some of it remains adhered to the substrate just on limited areas.

Fig. 8, on the other hand, illustrates a magnified view of one of the crack initiation sites identified as A in Fig. 7b. The dotted arrows indicate the propagation direction of a crack nucleated at site O, as determined from the convergence of such arrows at the substrate–coating interface. The secondary crack (SC) and one of the fracture steps (FST) indicated in Fig. 7b have also been pointed out.

The analysis of the cross section of this specimen, shown in Fig. 9, illustrates the presence of a number of primary cracks (identified as C), which run parallel to the fracture surface (FS), into the substrate. This observation confirms the nucleation and simultaneous propagation of a number of cracks, under these loading conditions, whose joint action leads eventually to the final fracture of the sample. It is important to observe that extensive cracking within the coating itself has given rise to its partial delamination, leading to a progressive decrease in the coating thickness as the fracture surface is approached.

Fig. 10a and b illustrates a comparison of the fracture surfaces of an uncoated sample and a coated one tested also in air, but at a lower maximum alternating stress of 223 MPa. Fig. 10a shows the fracture surface of an uncoated sample tested at 225 MPa, which fractured after 894,800 cycles. Contrarily to Fig. 7a, the fracture surface of this specimen shows the presence of two dominant cracks whose origins are enclosed in the areas identified as A and B, which led to the displacement of the ductile fracture zone (DFZ) to the bottom part of the fracture surface, as indicated in the photomicrograph.

Fig. 10b, on the other hand, illustrates the fracture surface of the coated specimen, which fractured after 723,000 cycles. The fracture surface exhibits somewhat different features to those observed in Fig. 7b and clearly shows that the fatigue fracture occurred due to the propagation of a dominant crack, which gave rise to the displacement of the ductile fracture zone (DFZ) to the opposite side of the crack initiation site. The arrows on the micrograph indicate the direction of crack propagation. As observed at high maximum alternating stresses, extensive delamination of the coating and interfacial cracking can be seen.

A closer view of the area identified as A in Fig. 10b is presented in Fig. 11, in which the crack propagation direction has been indicated by the dotted arrows. The point of convergence of such lines would indicate the approximate location of the crack nucleation site. One can notice the absence of fracture steps, as those observed in Figs. 7b and 8, which supports the fact that a dominant crack has been responsible of the specimen fracture. Fig. 12 illustrates a cross section view of this sample in which the fracture surface (FS) is located on the left. It can be clearly observed that, although extensive delamination of the coating from the substrate has occurred, contrarily to the features observed on the cross section view shown in Fig. 9, there are no other primary cracks parallel to the dominant main crack that gave rise to the final fracture of the specimen.

Regarding the samples tested in the NaCl solution, Fig. 13a and b illustrates the representative fracture surfaces of both an uncoated and a coated sample tested at 270 MPa. The uncoated specimen

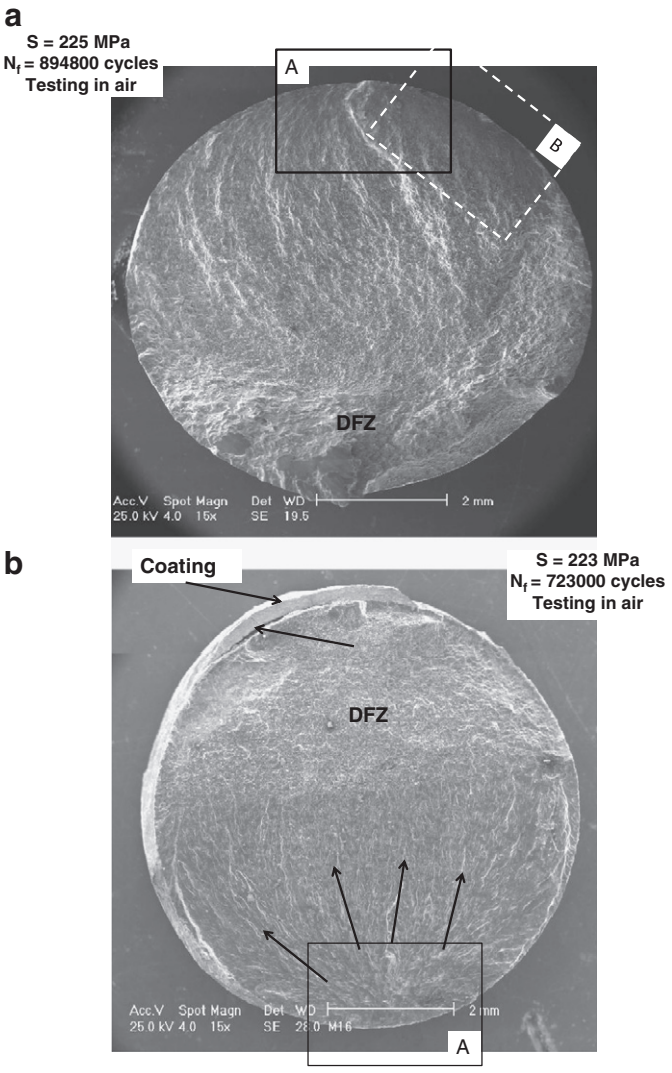

Fig. 10. (a) Fracture surface of an uncoated sample tested at 225 MPa, which failed after 894,800 cycles. (b) Fracture surface of a coated sample tested at 223 MPa, which failed after 723,000 cycles. The fatigue fracture of the coated specimen occurred due to the propagation of a dominant crack. Arrows on the micrograph indicate the direction of the crack propagation.

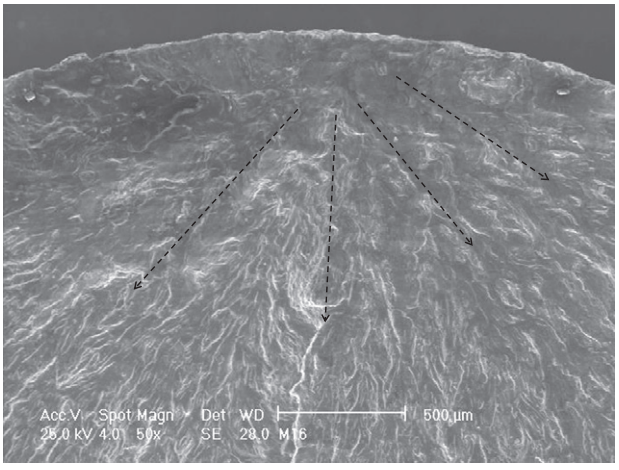

Fig. 11. Closer view of the area identified as A in Fig. 10b. The crack propagation direction has been indicated by the dotted arrows.

Please cite this article as: ES. Puchi-Cabrera, et al., Surf. Coat. Technol. (2012), doi:10.1016/j.surfcoat.2012.04.087

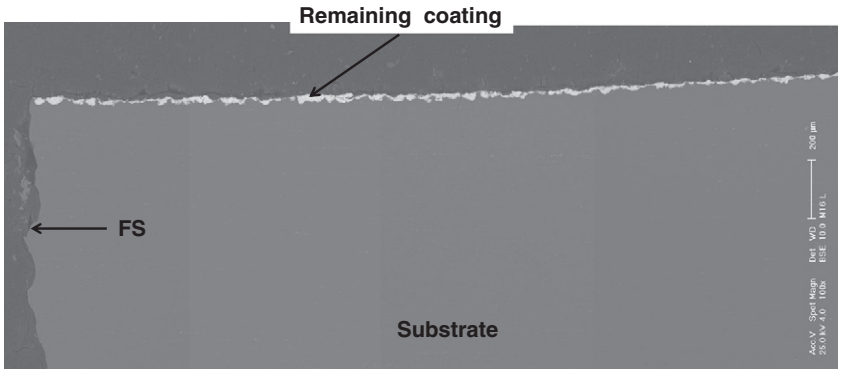

Fig. 12. Cross section view of the sample shown in Figs. 10b and 11. The fracture surface (FS) is located on the left. Extensive delamination of the coating from the substrate and the absence of other primary cracks, parallel to the dominant main crack that gave rise to the final fracture of the specimen, can be observed.

fractured after 78,800 cycles. Its fracture surface shown in Fig. 13a illustrates clearly that the fatigue fracture occurred as a consequence of the propagation of a dominant crack, whose origin is enclosed in the area identified as A, leading to the displacement of the DFZ to the opposite end of the fracture surface. On the contrary, the coated sample fractured after 112,700 cycles and the features observed on Fig. 13b are very similar to those already described for the coated sample tested in air at high stresses.

The fatigue fracture occurred due to the nucleation and simultaneous propagation of a number of cracks initiated at the substrate–coating interface. Such cracks, during their growth, consume a large part of the cross section of the specimen, giving rise to the displacement of the ductile fracture zone (DFZ), associated with final overloading, to the center of the sample. As it was indicated previously in relation to the specimens tested in air, under this testing medium, extensive delamination and interfacial cracking (I. C.) also take place, as indicated in this figure. It is important to notice that the differences found in the fractographic analysis between the uncoated and coated specimens can be interpreted in terms of the actual difference in the maximum alternating stresses at which both samples were tested, of approximately 54 MPa higher for the coated sample.

Fig. 14 illustrates a cross section view of this specimen, near the fracture surface (indicated as FS), which is shown on the right. On this composite photomicrograph, it can be clearly observed that during cyclic loading a number of primary fatigue cracks (identified as C) are nucleated along the gage length of the sample, some of which run parallel to the fracture surface, whereas others run at ~45° to the substrate–coating interface. Also, it can be observed that some of the cracks are nucleated at sharp notches and other geometrical irregularities that exist at the substrate–coating interface. However, it can be assumed that some of the cracks have been nucleated at the microstructural defects of the coating and that these are able to propagate along the coating and the substrate–coating interface, as well as into the substrate itself.

At lower alternating stresses, even under these corrosive conditions, the fracture surface of both the uncoated and coated specimens exhibited the dominance of a single crack, rather than the joint action of different cracks propagating from the periphery of the sample, as shown in Fig. 15a and b, respectively. In this case the specimens were tested at 175 MPa. The uncoated specimen failed after 1,012,600 cycles and, as shown in Fig. 15a, the fatigue fracture occurred as a consequence of the propagation of a single dominant crack, whose origin is enclosed in the area depicted as A. Similarly, the coated specimen fractured after 1,006,300 loading cycles and its fracture surface also clearly illustrates the displacement of the DFZ toward the opposite side of the single crack nucleation site. The crack propagation direction has been indicated by the dotted arrows on the micrograph.

Finally, Fig. 16 illustrates a cross section view of a specimen tested in air at a maximum alternating stress of 223 MPa, which achieved 5×10^6 cycles without fracture. It can be clearly observed that under

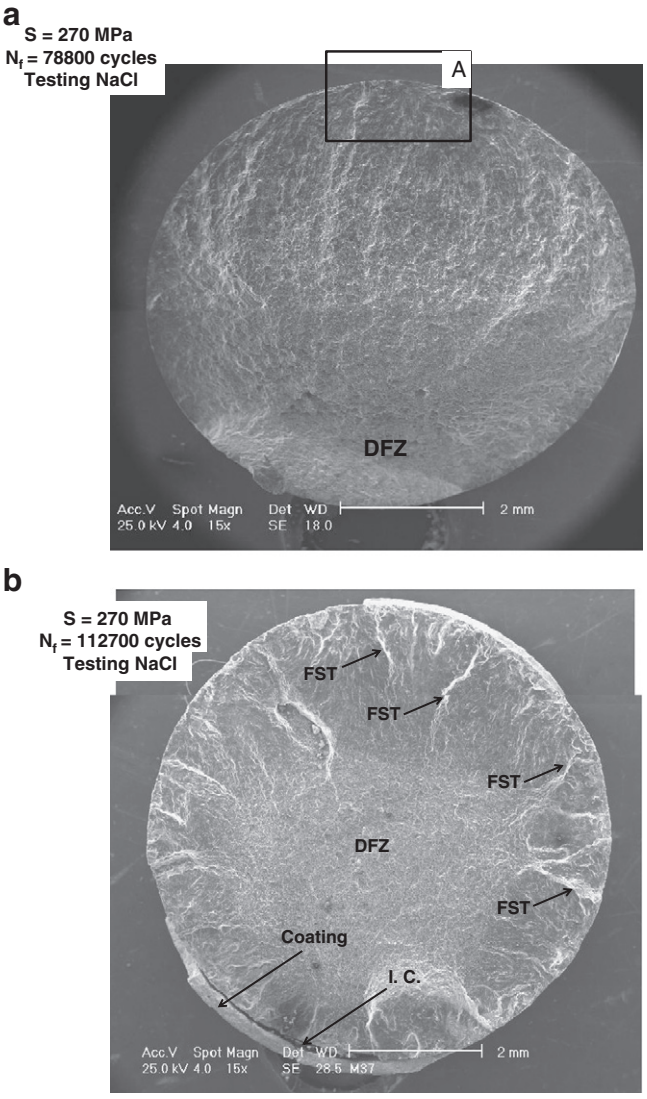

Fig. 13. (a) Fracture surface of an uncoated specimen tested in 3% NaCl solution at 270 MPa, which failed after 78,800 cycles. (b) Fracture surface of a coated specimen tested in 3% NaCl solution at 270 MPa, which failed after 112,700 cycles. It can be observed that the fatigue fracture of the coated sample occurred due to the nucleation and simultaneous propagation of a number of cracks initiated at the substrate–coating interface.

Please cite this article as: ES. Puchi-Cabrera, et al., Surf. Coat. Technol. (2012), doi:10.1016/j.surfcoat.2012.04.087

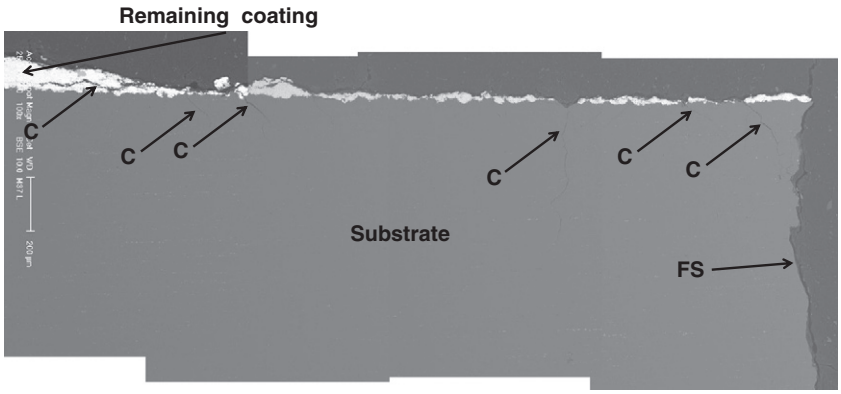

Fig. 14. Cross section view of this specimen shown in Fig. 13b. The fracture surface (FS) is located on the right. During cyclic loading a number of primary fatigue cracks (C) were nucleated along the gage length of the sample.

these loading conditions, the mechanical integrity of the coating is entirely preserved, as well as its adhesion to the substrate. There is not any visible evidence of delamination of the coating or of the existence of secondary cracks at the substrate–coating interface.

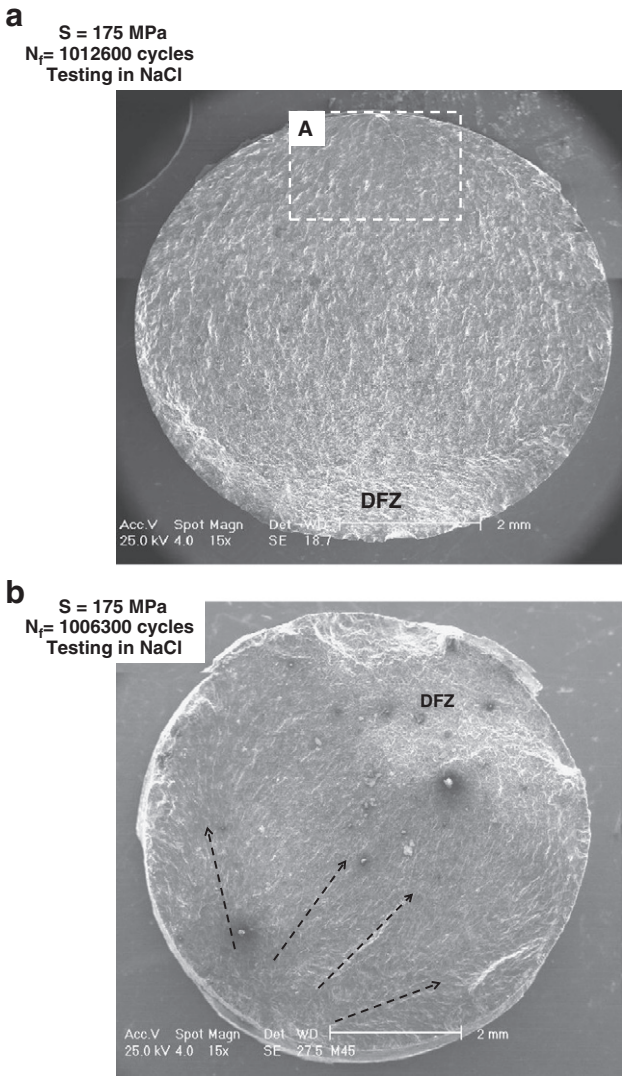

Fig. 15. (a) Fracture surface of an uncoated specimen tested in 3% NaCl solution at 175 MPa, which fractured after 1,012,600 loading cycles. (b) Fracture surface of a coated specimen tested in 3% NaCl solution at 175 MPa, which fractured after 1,006,300 loading cycles. The dominance of a single crack, responsible for the fatigue fracture in both samples, is clearly observed.

4. Discussion

The significant increase in fatigue properties of the coated system formed by the deposition of a WC–10Co–4Cr cermet onto the 7075-T6 aluminum alloy by HVOF thermal spray agrees quite well with the previous findings reported by Sartwell et al. [12,13] and Camargo et al. [14] for similar coated systems which involve the deposition of different carbides onto aluminum alloys of the 7000 series. The better fatigue and corrosion-fatigue performance of the coated system, in comparison with the uncoated substrate, arises both from the microstructural characteristics, corrosion resistance and mechanical properties of the coating, as well as from the deposition process itself.

It has been shown that the WC–10Co–4Cr cermet is a dense and quite homogeneous material with a high hardness, which is under a compressive residual stress field. However, given the significant plastic deformation at the substrate–coating interface shown in Fig. 4, it would be expected that the compressive residual stress field extends into the substrate material, providing a beneficial effect to the fatigue properties of the substrate–coating system. Such stress state hinders the propagation of fatigue cracks within the coating and therefore it has a beneficial effect on the mechanical integrity of the coated system. On the other hand, the different cross section views of the specimens shown in the previous section clearly indicate that the deposition of the coating gives rise to the plastic deformation of the substrate, which is also expected to induce a compressive residual

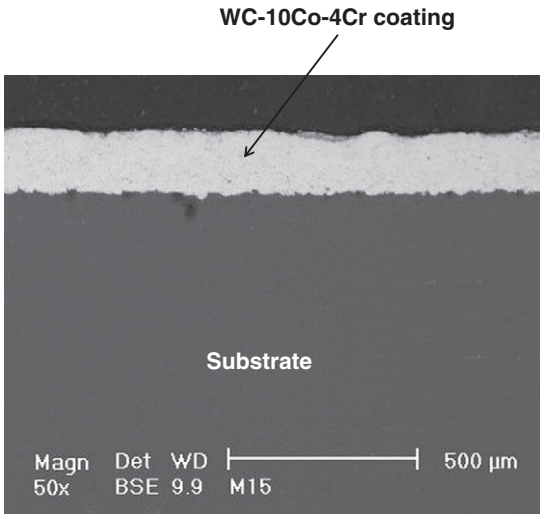

Fig. 16. Cross section view of a coated specimen tested in air at a maximum alternating stress of 223 MPa, which achieved 5×10^6cycles without fracture. The mechanical integrity coating has been entirely preserved, as well as its adhesion to the substrate.

Please cite this article as: ES. Puchi-Cabrera, et al., Surf. Coat. Technol. (2012), doi:10.1016/j.surfcoat.2012.04.087

stress state in the aluminum alloy, in the vicinity of the substrate–coating interface.

The fractographic analysis conducted on the fractured specimens indicated that fatigue cracks could either be nucleated and transferred from the coating to the substrate or nucleated at the sharp notches present at the interface, produced by plastic deformation by the impact of the coating particles during the first stages of deposition. In both cases, the presence of a residual stress field within the coating and in the substrate itself will benefit the fatigue strength of the coated system by reducing crack propagation rate. This view is further supported by the fact that at relatively low maximum alternating stresses, only a single dominant crack is responsible of the fatigue fracture of the coated system. This fact indicates that the stress intensity factor at the tip of other existing cracks, regardless of the location of their nucleation sites, is not high enough to induce their propagation, even under corrosive conditions.

When the samples are tested in air at maximum alternating stresses below ~225 MPa, the mechanical integrity of the coated system is entirely preserved since under this loading conditions fatigue cracks are not able to propagate, as shown in Fig. 16. A similar situation is observed when the specimens are tested at stresses below 125 MPa under the corrosive condition. Therefore, the lack of grit blasting prior to HVOF deposition does not seem to compromise the functionality of the coated system, while it avoids the introduction of further sharp stress concentrators for the nucleation of fatigue cracks.

At present, more experimental work is being carried out in order to analyze the fatigue behavior of the 7075-T6 aluminum alloy in the range of 10^6–10^7 cycles, which would provide a better basis for the comparison of the Wöhler curves of the coated system and the uncoated substrate.

5. Conclusions

The deposition of a WC–10Co–4Cr cermet by HVOF thermal spray onto a 7075-T6 aluminum alloy gives rise to a significant improvement of the fatigue strength of the coated system in comparison with the uncoated substrate. Such increase in fatigue performance is associated with microstructural characteristics, corrosion resistance and mechanical properties of the coating, as well as with the deposition process itself. The presence of a highly homogeneous, dense and hard coating under a compressive residual stress field, as well as the compressive residual stresses possibly induced in the substrate due to the plastic deformation that occurs during coating deposition, provides an explanation for the outstanding fatigue results that have been obtained. According to the present results, the lack of grit blasting prior to HVOF deposition does not seem to compromise the functionality of the coated system, while it avoids the introduction of further sharp stress concentrators for the nucleation of fatigue cracks. Therefore, it is concluded that from the fatigue behavior viewpoint, the WC–10Co–4Cr cermet constitutes a feasible replacement for electrolytic hard chromium plating.

Acknowledgments

The present investigation has been conducted with the financial support of the Scientific and Humanistic Development Council of the Universidad Central de Venezuela (CDCH-UCV) through the project PG-08-7775-2009/1. Professor Puchi-Cabrera gratefully acknowledges the financial support of the Conseil Régional Nord-Pas de Calais, France, through the International Chair program 2011. Professor Staia also acknowledges the financial support of the FONACIT-CNRS program through the project PI-2010000161.

References

[1] B. Cantor, H. Assender, P. Grant (Eds.), Aerospace Materials, Institute of Physics Publishing Ltd., Dirac House, Temple Back, Bristol BS1 6BE, ISBN: 0 7503 0742 0, 2001.
[2] J.G. Kaufman, Introduction to Aluminum Alloys and Tempers, ASM International, Materials Park OH, USA0-87170-689-X, 2000.
[3] G. Bolelli, L. Lusvarghi, R. Giovanardi, Surf. Coat. Technol. 202 (2008) 4793.
[4] G. Bolelli, L. Lusvarghi, M. Barletta, Surf. Coat. Technol. 202 (2008) 4839.
[5] J.A. Picas, A. Forn, G. Matthäus, Wear 261 (2006) 477.
[6] P.M. Natishan, S.H. Lawrence, R.L. Foster, J. Lewis, B.D. Sartwell, Surf. Coat. Technol. 130 (2000) 218.
[7] K.O. Legg, M. Graham, P. Chang, F. Rastagar, A. Gonzales, B. Sartwell, Surf. Coat. Technol. 81 (1996) 99.
[8] N. Serres, F. Hlawka, S. Costil, C. Langlade, F. Machi, A. Cornet, Surf. Coat. Technol. 204 (2009) 187.
[9] N. Serres, F. Hlawka, S. Costil, C. Langlade, F. Machi, A. Cornet, Surf. Coat. Technol. 204 (2009) 197.
[10] Directive 2000/53/EC of the European Parliament and of the Council of 18, September 2000 on end-of life vehicles.
[11] Directive 2002/95/EC of the European Parliament and of the Council of 27 January 2003 on the restriction of the use of certain hazardous substances in electrical and electronic equipment (RoHS) and directive 2002/96/EC on waste electrical and electronic equipment (WEEE).
[12] B.D. Sartwell, K.O. Legg, J. Schell, J. Sauer, P. Natishan, D. Dull, J. Falkowski, Validation of HVOF WC/Co Thermal Spray Coatings as a Replacement for Hard Chrome Plating on Aircraft Landing Gear, NRL/MR/6170-04-8762, Naval Research Laboratory, Washington, DC, USA, 2004.
[13] B.D. Sartwell, K.O. Legg, A. Nardi, R. Kestler, W. Assink, J. Schell, Replacement of Chromium Electroplating on C-2, E-2, P-3 and C-130 Propeller Hub Components Using HVOF Thermal Spray Coatings, NRL/MR/6170-04-8763, Naval Research Laboratory, Washington, DC, USA, 2004.
[14] J.A.M. Camargo, H.J. Cornelis, V.M.O.H. Cioffi, M.Y.P. Costa, Surf. Coat. Technol. 201 (2007) 9448.
[15] E.S. Puchi-Cabrera, R. Maccio, M.H. Staia, Surf. Eng. 22 (4) (2006) 253.
[16] M.Y.P. Costa, M.L.R. Venditti, H.J.C. Voorwald, M.O.H. Cioffi, T.G. Cruz, Mater. Sci. Eng., A 507 (2009) 29.
[17] E.S. Puchi-Cabrera, M.H. Staia, M.J. Ortiz-Mancilla, J.G. La Barbera-Sosa, E.A. Ochoa Pérez, C. Villalobos-Gutiérrez, S. Bellayer, M. Traisnel, D. Chicot, J. Lesage, Surf. Coat. Technol. 205 (2010) 1119.
[18] Y.Y. Santana, J.G. La Barbera-Sosa, J. Caro, E.S. Puchi-Cabrera, M.H. Staia, Surf. Eng. 24 (5) (2008) 374.
[19] Y.Y. Santana, J.G. La Barbera-Sosa, A. Bencomo, J. Lesage, D. Chicot, E. Bemporad, E.S. Puchi-Cabrera, M.H. Staia, Surf. Eng. (2011), http://dx.doi.org/10.1179/1743294411Y.0000000016.
[20] Y. Y. Santana, "Study of Mechanical and Tribological Properties of WC-based Materials", Ph. D. Thesis, School of Metallurgical Engineering and Materials Science, Faculty of Engineering, Universidad Central de Venezuela, 2008, D. L. No. lft4872008620742. Le Université des Science et Technologies de Lille, France, 2008.Ph. D. Thesis, 2008.
[21] E.S. Puchi-Cabrera, C. Villalobos-Gutierrez, I. Irausquin, J. La Barbera-Sosa, G. Mesmacque, Int. J. Fatigue 28 (2006) 1854.
[22] C.E. Stromeyer, Proc. R. Soc. Lond. Ser. A 90 (1914) 411.

Please cite this article as: ES. Puchi-Cabrera, et al., Surf. Coat. Technol. (2012), doi:10.1016/j.surfcoat.2012.04.087